International Journal of Control, 2013
Vol. 86, No. 7, 1292–1303, http://dx.doi.org/10.1080/00207179.2013.804951

Enforcing negative imaginary dynamics on mathematical system models

M.A. Mabrok[a,*], A. Lanzon[b], A.G. Kallapur[a] and I.R. Petersen[a]

[a]*School of Engineering and Information Technology, University of New South Wales at the Australian Defence Force Academy, Canberra, ACT 2600, Australia;* [b]*Control Systems Centre, School of Electrical and Electronic Engineering, University of Manchester, Manchester M13 9PL, United Kingdom*

(*Received 12 October 2012; final version received 25 April 2013*)

Flexible structures with collocated force actuators and position sensors lead to negative imaginary dynamics. However, in some cases, the mathematical models obtained for these systems, for example, using system identification methods may not yield a negative imaginary system. This paper provides two methods for enforcing negative imaginary dynamics on such mathematical models, given that it is known that the underlying dynamics ought to belong to this system class. The first method is based on a study of the spectral properties of Hamiltonian matrices. A test for checking the negativity of the imaginary part of a corresponding transfer function matrix is first developed. If an associated Hamiltonian matrix has pure imaginary axis eigenvalues, the mathematical model loses the negative imaginary property in some frequency bands. In such cases, a first-order perturbation method is proposed for iteratively collapsing the frequency bands whose negative imaginary property is violated and finally displacing the eigenvalues of the Hamiltonian matrix away from the imaginary axis, thus restoring the negative imaginary dynamics. In the second method, direct spectral properties of the imaginary part of a transfer function are used to identify the frequency bands where the negative imaginary properties are violated. A pointwise-in-frequency scheme is then proposed to restore the negative imaginary system properties in the mathematical model.

Keywords: negative imaginary systems; Hamiltonian matrices; pointwise frequency scheme

1. Introduction

Research on robust stability for various types of uncertain systems has received a great deal of interest in the control theory literature. For example, the work of Osvaldo Grasselli considers robust regulation, performance and tracking in the presence of uncertainties in physical parameters which affect all of the entries of the matrices describing the system to be controlled (Grasselli & Longhi, 1991; Grasselli, Longhi, & Tornambe, 1993; Grasselli, Longhi, Tornambe, & Valigi, 1996). Also, robust stability of interconnected systems has been studied under the notion of positive real (PR) system theory (Anderson & Vongpanitlerd, 1973; Brogliato, Lozano, Maschke, & Egeland, 2007). In general, systems that dissipate energy fall under the category of PR systems. For instance, they can arise in electric circuits with linear passive components and magnetic couplings. However, PR theory cannot be used in the presence of position and/or acceleration measurements (Petersen & Lanzon, 2010). This is a drawback concerning applications to the field of nanotechnology, especially for nano-positioning systems, where position measurements are widely used; see e.g. Bhikkaji and Moheimani (2009), Dong, Salapaka, and Ferreira (2007), Sebastian and Salapaka (2005), Salapaka, Sebastian, Cleveland, and Salapaka (2002), van Hulzen, Schitter, Van den Hof, and van Eijk (2010), Michellod, Mullhaupt, and Gillet (2006), Devasia, Eleftheriou, and Moheimani (2007), Messenger, Aten, McLain, and Howell (2009), El Rifai, El Rifai, and Youcef-Toumi (2004) and Diaz and mand Paul Reynolds (2012)

The notion of negative imaginary (NI) systems was first proposed in Lanzon and Petersen (2007, 2008) giving a robustness analysis result similar, in application, to the passivity theorem. NI systems are real-rational stable (possibly marginally stable) transfer function matrices that have a frequency response with an imaginary part that is negative for all frequencies. In NI systems theory, guarantees of robustness and stability involve the positive-feedback interconnection of an NI system and a strictly NI (SNI) system (Petersen & Lanzon, 2010). Hence, the results have similar applications to the small-gain theorem and the passivity theorem (Anderson & Vongpanitlerd, 1973; Brogliato et al., 2007). Here, the closed-loop system will be robust against uncertainty in the modal frequencies as well as unmodelled plant dynamics (Petersen & Lanzon, 2010).

NI systems theory has many engineering applications. Such classes of systems include DC machines (Engelken, Patra, Lanzon, & Petersen, 2010), electrical active filter circuits (Patra & Lanzon, 2011) and lightly damped structures

*Corresponding author. Email: m.mabrok@adfa.edu.au

(Fanson & Caughley, 1990; Moheimani, Vautier, & Bhikkaji, 2006; Petersen & Lanzon, 2010; Song, Lanzon, Patra, and Petersen, 2012; Xiong, Petersen, and Lanzon, 2012; Yong, Ahmed, and Moheimani, 2010). When force actuators and position sensors (such as piezoelectric sensors) are collocated on a flexible structure, the input/output map must be NI (Petersen & Lanzon, 2010). Stability results for interconnected systems with an NI frequency response have been applied to the decentralised control of large vehicle platoons in Cai and Hagen (2010). van der Schaft (2011) shows that the class of linear systems having NI transfer function matrices is a direct extension of the class of linear Hamiltonian input–output systems. Also, an extension of NI systems to infinite-dimensional systems has been studied in Opmeer (2011) and a single-input single-output (SISO) generalisation to nonlinear systems is considered in Angeli (2006).

Precise modelling of structural dynamics is often difficult as it is sensitive to boundary conditions and environmental effects. Therefore, using force actuators combined with collocated measurements of velocity, position or acceleration can improve the performance of control systems by increasing damping and by restricting the dynamical properties via collocation (Petersen & Lanzon, 2010). Here, collocated means that sensors and actuators have the same location and direction. Since flexible structures with collocated force actuators and position sensors are typically SNI, NI systems theory can be effectively applied to these systems (Petersen & Lanzon, 2010). Also, it has been shown in Lanzon and Petersen (2008) that a necessary and sufficient condition for the internal stability of the positive-feedback interconnection of an NI and an SNI system is for the overall open-loop DC gain to be less than unity.

For systems involving flexible structure dynamics, it may be difficult to obtain an exact system model by constructing differential equations from first principles. An alternative method for obtaining a mathematical system model is by means of system identification. However, the resulting mathematical model may not exactly describe the true dynamics of the underlying system, especially under noisy measurements. In such cases the identified system models can sometimes lead to mathematical models that do not reflect the actual characteristics of the underlying system. For example, the process of system identification when applied to linear time-invariant (LTI) systems which are known to be NI might lead to a model which is not NI. In such cases, the system model should be perturbed to enforce the underling NI dynamics. In this paper, we achieve such an NI enforcement by extending results from the theory of passivation for LTI systems; see e.g. Chinea and Grivet-Talocia (2007, 2008) and Grivet-Talocia (2004).

This paper is further organised as follows. Section 2 recalls the definitions of NI systems. In Section 3, an algebraic procedure is presented that allows us to pinpoint the frequency bands where the NI property is violated. Section 4 describes two schemes used to enforce the mathematical model to be NI: one based on a Hamiltonian perturbation scheme and the other based on a discrete frequency scheme. In Section 5, we present a practical example involving an optical cavity system. Section 6 concludes the paper with a note on open problems.

2. Preliminaries

The notion of NI transfer functions and several related results developed in Lanzon and Petersen (2008) and Xiong, Petersen, and Lanzon (2010) are now recalled.

Definition 2.1 (Xiong et al., 2010)**:** A square transfer function matrix $G(s)$ is NI if the following conditions are satisfied.

(1) $G(s)$ has no pole at the origin and in $\mathrm{Re}[s] > 0$.
(2) For all $\omega > 0$ such that $j\omega$ is not a pole of $G(s)$, $j(G(j\omega) - G(j\omega)^*) \geq 0$.
(3) If $j\omega_0$ with $\omega_0 > 0$ is a pole of $G(s)$, then it is at most a simple pole and the residue matrix $K_0 = \lim_{s \to j\omega_0}(s - j\omega_0)sG(s)$ is positive semi-definite Hermitian.

Lemma 2.2 (Lanzon and Petersen, 2008; Xiong et al., 2010)**:** *Let* $\left[\begin{array}{c|c} A & B \\ \hline C & D \end{array}\right]$ *be a minimal state-space realisation of a transfer function matrix G(s). Then G(s) is NI if and only if det(A)* $\neq$ *0,* $D = D^T$ *and there exists a real matrix* $Y > 0$ *such that*

$$AY + YA^* \leq 0 \text{ and } \mathrm{B} = -\mathrm{AYC}^*. \tag{1}$$

The above lemma is termed as 'the negative-imaginary lemma'. An SNI system is defined as follows.

Definition 2.3 (Lanzon and Petersen, 2008; Xiong et al., 2010)**:** A square transfer function matrix $G(s)$ is SNI if the following conditions are satisfied.

1. $G(s)$ has no pole in $\mathrm{Re}[s] \geq 0$.
2. For all $\omega > 0, j(G(j\omega) - G(j\omega)^*) > 0$.

Note that the strict condition $j(G(j\omega) - G(j\omega)^*) > 0$ is always violated at $\omega = 0$ as $G(0) = G(0)^T$. A strongly SNI lemma without minimality assumptions is given in Lanzon, Song, Patra, and Petersen (2011) and a weakly SNI lemma is given in Xiong et al. (2010).

3. Characterisation of frequency bands where the negative imaginary frequency domain property is violated

In this section, we describe two algebraic procedures that allow us to pinpoint frequency bands where the NI property

is violated; i.e. frequency bands where $j(G(j\omega) - G(j\omega)^*)$ is not positive semi-definite.

3.1 First method (Hamiltonian-based method)

In this method, we use a Hamiltonian-type matrix to check for violations of the NI frequency domain property of a transfer function matrix.

Theorem 3.1: *Given a transfer function matrix G(s) with minimal state-space realisation* $\left[\begin{array}{c|c} A & B \\ \hline C & D \end{array}\right]$, *assume A has no pure imaginary axis eigenvalues,* $D = D^T$, $CB + B^TC^T > 0$, *and* $\delta \leq 0$ *is not an eigenvalue of* $\frac{-1}{2}(CB + B^TC^T)$. *Then given* $\omega_0 \neq 0$, $\delta \in \lambda(T(j\omega_0))$ *if and only if* $j\omega_0 \in \lambda(N_\delta)$. *Here,* $\lambda(\cdot)$ *denotes the spectrum of the matrix* $(\cdot)$, $T(j\omega) = \frac{-j\omega}{2}(G(j\omega) - G(j\omega)^*)$ *and the Hamiltonian matrix* N_δ *is defined by*

$$N_\delta = \begin{bmatrix} A + BQ_\delta^{-1}CA & BQ_\delta^{-1}B^T \\ -A^TC^TQ_\delta^{-1}CA & -A^T - A^TC^TQ_\delta^{-1}B^T \end{bmatrix}, \quad (2)$$

with $Q_\delta = -2\delta I - CB - B^TC^T$.

Proof: Since $\left[\begin{array}{c|c} A & B \\ \hline C & D \end{array}\right]$ is a minimal state-space realisation of the transfer function matrix $G(s)$, it follows that the transfer function matrix $H(s) = s(G(s) - D)$ has a minimal state-space realisation $\left[\begin{array}{c|c} A & B \\ \hline CA & CB \end{array}\right]$.

Now, $\delta \in \lambda(T(j\omega_0))$, where $\omega_0 \neq 0$ if and only if there exists non-zero vector $u \in \mathbb{C}^m$ such that

$$\begin{aligned} T(j\omega_0)u = \delta u, &\Leftrightarrow \frac{-1}{2} j\omega_0(G(j\omega_0) - G(j\omega_0)^*)u = \delta u, \\ &\Leftrightarrow (CA(j\omega_0 I - A)^{-1}B \\ &\quad + B^T(-j\omega_0 I - A^T)^{-1}A^TC^T \\ &\quad + CB + B^TC^T)u = -2\,\delta u, \\ &\Leftrightarrow (CAr + B^Ts) + (CB + B^TC^T)u = -2\,\delta u, \end{aligned} \quad (3)$$

where

$$r = (j\omega_0 I - A)^{-1}Bu \text{ and} \quad (4)$$

$$s = (-j\omega_0 I - A^T)^{-1}A^TC^Tu. \quad (5)$$

Note that $\left[\begin{smallmatrix} r \\ s \end{smallmatrix}\right]$ must be non-zero since if $\left[\begin{smallmatrix} r \\ s \end{smallmatrix}\right] = 0$, it follows from (3) that $(CB + B^TC^T)u = -2\delta u$, which contradicts the assumption that δ is not an eigenvalue of the matrix $\frac{-1}{2}(CB + B^TC^T)$.

Now (3) is equivalent to

$$\begin{aligned} &\begin{bmatrix} CA & B^T \end{bmatrix}\begin{bmatrix} r \\ s \end{bmatrix} = Q_\delta u, \\ &\Leftrightarrow Q_\delta^{-1}\begin{bmatrix} CA & B^T \end{bmatrix}\begin{bmatrix} r \\ s \end{bmatrix} = u, \end{aligned} \quad (6)$$

where $Q_\delta = -2\,\delta I - CB - B^TC^T$. Note that Q_δ must be invertible since we have assumed that δ is not an eigenvalue of the matrix $\frac{-1}{2}(CB + B^TC^T)$. Also, (4) and (5) can be written as

$$\begin{aligned} &Bu = (j\omega_0 I - A)r,\ A^TC^Tu = (-j\omega_0 I - A^T)s \\ &\Leftrightarrow \begin{bmatrix} B \\ -A^TC^T \end{bmatrix}u = j\omega_0\begin{bmatrix} r \\ s \end{bmatrix} + \begin{bmatrix} -A & 0 \\ 0 & A^T \end{bmatrix}\begin{bmatrix} r \\ s \end{bmatrix}. \end{aligned} \quad (7)$$

Thus, substituting (6) into (7), we obtain

$$\begin{aligned} &\begin{bmatrix} B \\ -A^TC^T \end{bmatrix}Q_\delta^{-1}\begin{bmatrix} CA & B^T \end{bmatrix}\begin{bmatrix} r \\ s \end{bmatrix} \\ &= j\omega_0\begin{bmatrix} r \\ s \end{bmatrix} + \begin{bmatrix} -A & 0 \\ 0 & A^T \end{bmatrix}\begin{bmatrix} r \\ s \end{bmatrix} \quad (8) \\ &\Leftrightarrow \begin{bmatrix} B \\ -A^TC^T \end{bmatrix}Q_\delta^{-1}\begin{bmatrix} CA & B^T \end{bmatrix}\begin{bmatrix} r \\ s \end{bmatrix} \\ &\quad + \begin{bmatrix} A & 0 \\ 0 & -A^T \end{bmatrix}\begin{bmatrix} r \\ s \end{bmatrix} = j\omega_0\begin{bmatrix} r \\ s \end{bmatrix} \quad (9) \\ &\Leftrightarrow N_\delta\begin{bmatrix} r \\ s \end{bmatrix} = j\omega_0\begin{bmatrix} r \\ s \end{bmatrix}. \quad (10) \end{aligned}$$

Thus, $\delta \in \lambda(T(j\omega_0))$ if and only if $j\omega_0 \in \lambda(N_\delta)$, where

$$N_\delta = \begin{bmatrix} A + BQ_\delta^{-1}CA & BQ_\delta^{-1}B^T \\ -A^TC^TQ_\delta^{-1}CA & -A^T - A^TC^TQ_\delta^{-1}B^T \end{bmatrix}.$$

This completes the proof of Theorem 3.1. □

Theorem 3.1 allows us to compute the frequencies at which the eigenvalues of the imaginary part of a transfer function matrix cross or touch any given threshold (or critical level) $\delta = \delta_0$. A test for checking the frequency domain inequality of NI systems can be readily obtained by using the critical level $\delta_0 = 0$.

To illustrate this theorem, consider the situation depicted in Figure 1. This plot describes the eigenvalues of $T(j\omega) = \frac{-j\omega}{2}(G(j\omega) - G(j\omega)^*)$, where $G(s) = \frac{2s+1}{s^2+3s+3}$ (in this case there is only one eigenvalue equal to the value of the SISO frequency response $T(j\omega)$). $G(s)$ loses the NI property in the shaded frequency band from ω_0 to ω_1 as the frequency domain inequality for the imaginary part is not fulfiled. The number of pure imaginary axis eigenvalues for positive frequencies of the associated Hamiltonian matrix is two, which corresponds to frequencies $\omega_0 = 0$ and ω_1. The positive frequency axis is therefore subdivided into two frequency bands: (ω_0, ω_1) and (ω_1, ∞).

From this example, we observe that using only the number of pure imaginary axis eigenvalues of N_0 is not enough to allow us to determine whether $T(j\omega) \leq 0$ or not (meaning that whether the frequency domain inequality on the imaginary part of $G(j\omega)$ is negative or not) in each

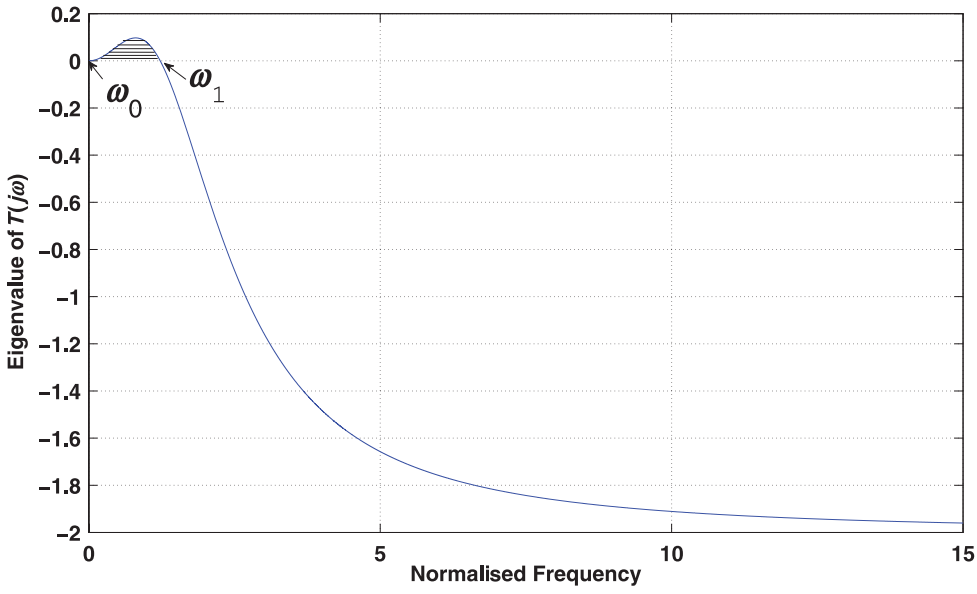

Figure 1. Eigenvalue distribution versus normalised frequency for $T(j\omega) = \frac{-j\omega}{2}(G(j\omega) - G(j\omega)^*)$, with $G(s) = \frac{2s+1}{s^2+3s+3}$.

frequency band. In order to obtain such a characterisation, we need to also consider the slope of the eigenvalue curve at points crossing the critical level $\delta = 0$. Since the eigenvalues are continuous functions of frequency, the number of successive crossings with positive (or negative) slopes can be precisely related to the number of eigenvalues crossing the threshold in each frequency band.

To find the slope of the eigenvalue at a crossing point, assume that $\bar{\lambda}$ is the largest eigenvalue of $T(j\omega)$ and u is the corresponding right eigenvector. Then we have

$$(T(j\omega) - \bar{\lambda} I)u = 0. \tag{11}$$

Differentiating (11) with respect to the frequency ω and multiplying by the left eigenvector v^T, we obtain the following equation:

$$\frac{d\bar{\lambda}}{d\omega} = \frac{v^T \frac{d}{d\omega} T(j\omega) u}{v^T u}. \tag{12}$$

Note that $\frac{d}{d\omega} T(j\omega)$ can be easily computed from the state-space data of $T(s)$.

From (12), we can obtain the sign for the slope of the largest eigenvalue at the crossing points. The frequency bands where the NI property is violated can be determined by collecting the pure imaginary axis eigenvalues with positive frequency of the Hamiltonian matrix N_δ in (2) with $\delta = 0$, then sorting the frequencies of these eigenvalues in the order of $\omega_0 = 0 < \omega_1 < \omega_2 < \cdots < \omega_K$ (assuming that all eigenvalues at the frequency ω_i have multiplicity one). Next, evaluate the slope in (12) for each eigenvalue at frequency ω_i where (i =1:K), starting from ω_K and counting the number of negative and positive signs of the slopes. Note that $G(j\omega)$ is assumed to satisfy the NI condition as $\omega \to +\infty$. This implies that $CB + B^T C^T > 0$, which ensures that the sign of the slope at ω_K is negative. In order to find the first frequency region where the NI property violation occurs, we start from ω_K and count the number of positive and negative slopes as we work back towards ω_0. When the number of positive and negative slopes becomes equal, then the first region of local NI property violation has been found. Also, if the number of negative slopes is greater than that of positive slopes from ω_K to ω_0, this implies that frequency domain NI condition is violated for all $\omega \in (0, \omega_K)$.

3.2 Second method

The Hamiltonian-based method proposed in Section 3.1 can be used only when the matrix $CB + B^T C^T$ is non-singular, which means that the relative degree should always be one. In the method outlined in this section, we consider a general case by relaxing the singularity assumption on the matrix $CB + B^T C^T$.

Theorem 3.2: *Given a transfer function matrix G(s) having no poles in* $\mathrm{Re}[s] \geq 0$, $D = D^T$ *and let G(s) have a minimal state-space realisation* $\left[\begin{array}{c|c} A & B \\ \hline C & D \end{array}\right]$. *Also, suppose that* $\beta < 0$. *Then* β *is an eigenvalue of* $H(j\omega_0) = \frac{-j}{2}(G(j\omega_0) - G(j\omega_0)^*)$ *if and only if* $j\omega_0$ *is an eigenvalue of the matrix*

$$M_\beta = j(2\beta)^{-1} \begin{bmatrix} B \\ -C^T \end{bmatrix} \begin{bmatrix} -C & B^T \end{bmatrix} + \begin{bmatrix} A & 0 \\ 0 & -A^T \end{bmatrix}. \tag{13}$$

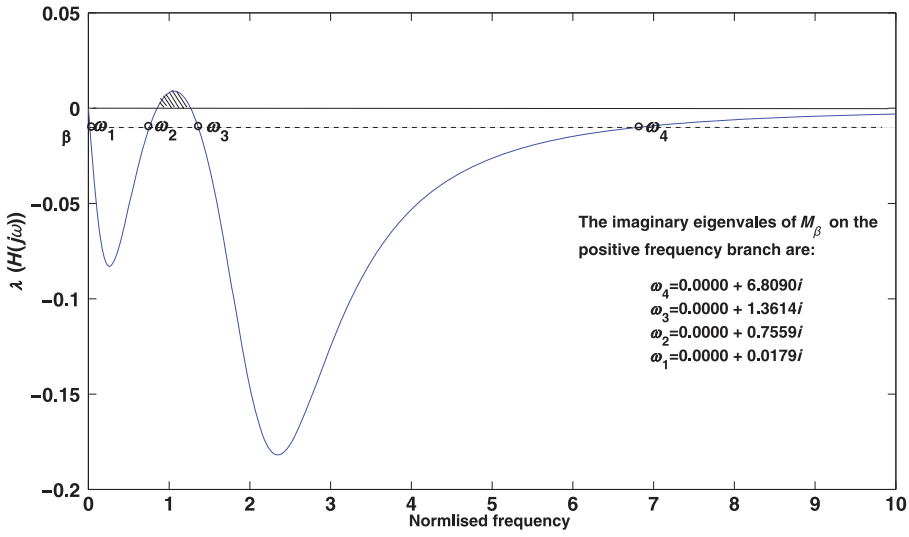

Figure 2. The eigenvalues of $H(j\omega) = \frac{-j}{2}(G(j\omega) - G(j\omega)^*)$ cross the threshold $\beta = -0.01$ four times at $\omega_1, \omega_2, \omega_3$ and ω_4.

Proof: Assume that β is an eigenvalue of $H(j\omega_0)$, then there exists a non-zero vector u such that

$$\begin{aligned} H(j\omega_0)u = \beta u &\Leftrightarrow \frac{-j}{2}(G(j\omega_0) - G(j\omega_0)^*)u = \beta u \\ &\Leftrightarrow -j(C(j\omega_0 I - A)^{-1}B - B^T \\ &\quad \times (-j\omega_0 I - A^T)^{-1}C^T)u = 2\beta u \\ &\Leftrightarrow -j(Cr - B^T s) = 2\beta u \qquad (14) \end{aligned}$$

$$\Leftrightarrow j(2\beta)^{-1}\begin{bmatrix} -C & B^T \end{bmatrix}\begin{bmatrix} r \\ s \end{bmatrix} = u, \qquad (15)$$

where

$$\begin{aligned} r &= (j\omega_0 I - A)^{-1}Bu \text{ and} \\ s &= (-j\omega_0 I - A^T)^{-1}C^T u. \end{aligned} \qquad (16)$$

Note that $\begin{bmatrix} r \\ s \end{bmatrix} \neq 0$ since if it were equal to zero, it would contradict $u \neq 0$ via (14).

Also, (16) can be written as

$$\begin{bmatrix} B \\ -C^T \end{bmatrix}u = j\omega_0\begin{bmatrix} r \\ s \end{bmatrix} + \begin{bmatrix} -A & 0 \\ 0 & A^T \end{bmatrix}\begin{bmatrix} r \\ s \end{bmatrix}. \qquad (17)$$

Substituting (15) into (17) we obtain

$$\begin{aligned} &\begin{bmatrix} B \\ -C^T \end{bmatrix}j(2\beta)^{-1}\begin{bmatrix} -C & B^T \end{bmatrix}\begin{bmatrix} r \\ s \end{bmatrix} \\ &= j\omega_0\begin{bmatrix} r \\ s \end{bmatrix} + \begin{bmatrix} -A & 0 \\ 0 & A^T \end{bmatrix}\begin{bmatrix} r \\ s \end{bmatrix} \\ &\Leftrightarrow j(2\beta)^{-1}\begin{bmatrix} B \\ -C^T \end{bmatrix}\begin{bmatrix} -C & B^T \end{bmatrix}\begin{bmatrix} r \\ s \end{bmatrix} + \begin{bmatrix} A & 0 \\ 0 & -A^T \end{bmatrix}\begin{bmatrix} r \\ s \end{bmatrix} \\ &= j\omega_0\begin{bmatrix} r \\ s \end{bmatrix} \Leftrightarrow M_\beta\begin{bmatrix} r \\ s \end{bmatrix} = j\omega_0\begin{bmatrix} r \\ s \end{bmatrix}. \qquad (18) \end{aligned}$$

This shows that $j\omega_0$ is an eigenvalue of M_β and proves the necessary part of the theorem.

In order to prove sufficiency, suppose that M_β has an eigenvalue of $j\omega_0$. Then (18) holds for some $\begin{bmatrix} r \\ s \end{bmatrix} \neq \begin{bmatrix} 0 \\ 0 \end{bmatrix}$. We can then define a vector u as in (15),

which implies that β is an eigenvalue of $H(j\omega_0)$. Note that $u \neq 0$ because if it were equal to zero, then via (17) $\begin{bmatrix} r \\ s \end{bmatrix}$ would also need to be equal to zero. This would contradict the minimality of the realisation, since A has no eigenvalues on $j\omega$ axis. This completes the proof. □

According to Theorem 3.2, if the matrix M_β has a pure imaginary axis eigenvalue, this implies that $H(j\omega)$ has an eigenvalue crossing the threshold β. To illustrate this, consider the following example. Suppose that

$$G(s) = \frac{2s^2 + s + 1}{2s^4 + 7s^3 + 17s^2 + 18s + 5}. \qquad (19)$$

The corresponding M_β for $G(s)$ with $\beta = -0.01$ has four pure imaginary axis eigenvalues on the positive frequency branch as shown in Figure 2. This implies that the eigenvalues of $H(j\omega) = \frac{-j}{2}(G(j\omega) - G(j\omega)^*)$ cross the threshold $\beta = -0.01$ four times at $\omega_1, \omega_2, \omega_3$and ω_4.

This information is insufficient in determining the frequency bands where the frequency domain inequality ensuring NI part is violated. However, since the eigenvalues

of $H(j\omega)$ are continuous functions of ω, the slope of the tangent at the points where the maximum eigenvalue of $(H(j\omega))$ crosses the threshold β can be used to determine the frequency bands where $H(j\omega) - \beta I$ is not negative semi-definite. In the above example, $H(j\omega) + 0.01I$ is not negative semi-definite in the frequency bands $(0, \omega_1)$, (ω_2, ω_3) and (ω_3, ∞).

Now, since $\beta < 0$, we cannot guarantee that $H(j\omega)$ is not negative semi-definite (i.e. where NI property is violated) for those frequency bands that satisfy $H(j\omega)) - \beta I$ is not negative semi-definite. We can avoid this problem by computing the maximum eigenvalue in this frequency band according to

$$\max_{\omega\in(\omega_i,\omega_k)} \overline{\lambda}(H(j\omega)), \tag{20}$$

where $\overline{\lambda}(\cdot)$ denotes the largest eigenvalue in the set $\lambda(\cdot)$, and ω_i and ω_k are the boundaries for the frequency bands that satisfy that $H(j\omega) - \beta I$ is not negative semi-definite. The problem in (20) converges quickly as it is a line search associated with only one variable with a good initial guess (the midpoint of ω_i and ω_k).

By solving the problem in (20), if $\max_{\omega\in(\omega_i,\omega_k)} \overline{\lambda}(H(j\omega)) > 0$, then a violation of the NI frequency domain property occurs between ω_i and ω_k. Also, if $\max_{\omega\in(\omega_i,\omega_k)} \overline{\lambda}(H(j\omega)) < 0$, this implies that $G(s)$ satisfies $j(G(j\omega) - G(j\omega)^*) > 0$ between ω_i and ω_k, and if $\max_{\omega\in(\omega_i,\omega_k)} \overline{\lambda}(H(j\omega)) = 0$, it implies that $G(s)$ satisfies $j(G(j\omega) - G(j\omega)^*) \geq 0$ between ω_i and ω_k.

It is important to note that we have to choose β as small as possible as $\lim_{\omega\to 0} H(j\omega) = 0$ and $\lim_{\omega\to\infty} H(j\omega) = 0$. This implies that irrespective of the smallness of the value of β, $\overline{\lambda}(H(j\omega))$ will cross the β threshold at some small frequency ω_0 and at some large frequency ω_n. So, the idea is to choose β sufficiently small such that $\omega_0 < \widetilde{\omega_L}$ and $\omega_n > \widetilde{\omega_H}$, where $[\widetilde{\omega_L}, \widetilde{\omega_H}]$ is the largest frequency range of interest.

4. Enforcing a system model to be negative imaginary

In this section, we address the problem of finding an approximate NI system model for a given stable but non-negative imaginary system model due to violation of the frequency domain inequality in some frequency bands. To do so, we will present two different perturbation schemes: the Hamiltonian perturbation scheme and the discrete frequency scheme. These two perturbation schemes have been selected based on the comparative study in Grivet-Talocia and Ubolli (2008).

4.1 Hamiltonian perturbation scheme

Let us consider a controllable state-space representation for $\Sigma(s)$ as

$$\dot{x}(t) = Ax(t) + Bu(t), \tag{21}$$

$$y(t) = Cx(t) + Du(t), \tag{22}$$

where $A \in \mathbb{R}^{n\times n}$, $B \in \mathbb{R}^{n\times m}$, $C \in \mathbb{R}^{m\times n}$ and $D \in \mathbb{R}^{m\times m}$. Also, assume that $CB + B^TC^T > 0$, which ensures that $G(s)$ satisfy the NI property where $s \to +\infty$. The aim is to find a perturbed state-space realisation $\Sigma_p(s)$ which is NI.

Since Σ is assumed to be stable, the corresponding A matrix will remain the same in the perturbed model $\Sigma_p(s)$. Now if we consider a perturbed model $\Sigma_p(s)$ by only altering the C matrix in (28), we obtain a state-space realisation for $\Sigma_p(s)$ given by

$$\dot{x}(t) = Ax(t) + Bu(t), \tag{23}$$

$$y_p(t) = C_px(t) + Du(t). \tag{24}$$

The state-space realisation of the transfer function $s(\Sigma(s) - D)$ is given as

$$\dot{x}(t) = Ax(t) + Bu(t), \tag{25}$$

$$\bar{y}(t) = \bar{C}x(t) + \bar{D}u(t), \tag{26}$$

where $\bar{C} = CA$ and $\bar{D} = CB$, and the state-space realisation for the perturbed model $s(\Sigma_p(s) - D)$ is given by

$$\dot{x}(t) = Ax(t) + Bu(t), \tag{27}$$

$$\bar{y_p}(t) = \bar{C}_px(t) + \bar{D}_pu(t), \tag{28}$$

where the matrices $\bar{C_p} = C_pA$ and $\bar{D_p} = C_pB$. Then the discrepancies $d\bar{C}$ and $d\bar{D}$ are given by

$$d\bar{C} = \bar{C}_p - \bar{C} = (C_p - C)A = dC\ A, \tag{29}$$

$$d\bar{D} = \bar{D}_p - \bar{D} = (C_p - C)B = dC\ B. \tag{30}$$

Let X be a matrix whose columns span the kernel space of B^T, i.e. $B^TX = 0$. Then setting $dC = \Phi X^T$, where Φ is an arbitrary square matrix to be determined, results in $d\bar{D} = 0$.

The difference in the impulse response of the two systems induced by this perturbation is expressed as

$$dh(t) = L^{-1}\{s(\Sigma(s) - D) - s(\Sigma_p(s) - D)\} = d\bar{C}(e^{At}B). \tag{31}$$

The matrix $C_p = C + \Phi X^T$ is chosen to minimise the cumulative energy of the impulse response discrepancy $dh(t)$ which can be computed as follows:

$$E = \mathrm{tr}(d\bar{C}\ W\ d\bar{C}^T), \tag{32}$$

where W is the controllability Gramian of the pair (A, B) (Brockett, 1970), which can be computed as a unique symmetric and positive definite solution of the Lyapunov equation

$$AW + WA = BB^T. \tag{33}$$

Then, substituting (29) into (32) gives

$$E = \mathrm{tr}(dC\ A\ W\ A^T\ dC^T) = \mathrm{tr}(\Phi\ X^T\ A\ W\ A^T\ X\ \Phi^T). \tag{34}$$

Since X^TAWA^TX is a positive definite matrix, it can be factorised using Cholesky decomposition as $X^T A\, W A^T X = K^T K$. Now, we can define $\Phi_k = \Phi K^T$. This leads to

$$E = \mathrm{tr}(\Phi_k \Phi_k^T) = \| \Phi_k \|_F^2 = \| \mathrm{vec}(\Phi_k) \|_2^2, \tag{35}$$

where vec(Π) denotes a vector obtained by stacking columns of the matrix Π, $\| \cdot \|_F^2$ denotes the Frobenius norm and $\| \cdot \|_2^2$ denotes the vector Euclidean norm.

Now, we apply a first-order perturbation to the Hamiltonian matrix N_0 (N_δ in (2) with $\delta = 0$) in order to move the pure imaginary axis eigenvalues off the $j\omega$-axis. Since $C_p = C + \Phi X^T$, it follows that $C_pB = CB$ and hence $Q_0 = -C_pB - B^TC_p^T = -CB - B^TC^T$ remains unchanged when C changes. The perturbation of the Hamiltonian matrix N_0 induced by small perturbations in the state matrix C is given by

$$N_0|_p = N_0 + dN_0, \tag{36}$$

where a first-order approximation is given by

$$dN_0 \approx \begin{bmatrix} BQ_0^{-1}\Phi X^T A & \\ A^TC^TQ_0^{-1}\Phi X^TA + A^TX\Phi^TQ_0^{-1}CA & \\ & 0 \\ & -A^TX\Phi^TQ_0^{-1}B^T \end{bmatrix}.$$

Now we find the matrix Φ in order to displace all pure imaginary eigenvalues $j\omega_i$ to a new location $j\omega_{i,p}$, where

$$j\omega_{i,p} - j\omega_i \simeq \frac{\upsilon_i^*\, J\ dN_0\ \upsilon_i}{\upsilon_i^* J \upsilon_i}, \tag{37}$$

with $J = \left[\begin{smallmatrix} 0 & I \\ -I & 0 \end{smallmatrix}\right]$, and υ_i is the corresponding eigenvector for ω_i of the Hamiltonian matrix N_0 corresponding to the eigenvalue $j\omega$.

With some algebraic manipulation (e.g. see Grivet-Talocia, 2004), (37) can be expressed as

$$\begin{aligned} &2\mathfrak{Re}((\upsilon_{i1}^TA^TXK^{-1}) \otimes z_i^*)\mathrm{vec}(\Phi_k) \\ &\quad = -\mathfrak{Im}(\upsilon_i^* J \upsilon_i)(j\omega_{i,p} - j\omega_i), \end{aligned} \tag{38}$$

where

$$z_i = -Q_0^{-1}B^T\upsilon_{i2} - Q_0^{-1}CA\upsilon_{i1}. \tag{39}$$

Here, $(\upsilon_{i1}, \upsilon_{i2})$ is a partition of the eigenvector υ_i using the induced block partition of the Hamiltonian matrix, $\otimes$ is the Kronecker product, and $\mathfrak{Re}(\cdot)$ and $\mathfrak{Im}(\cdot)$ are the real and imaginary parts. The output matrix perturbation Φ_k that is required to move the pure imaginary axis eigenvalues $j\omega_i$ to $j\omega_{i,p}$ must satisfy the linear constraint (38). In summary, these constraints can be described as a standard least-squares problem

$$\min \|\mathrm{vec}(\Phi_k)\|_2 \text{ subject to } Z\ \mathrm{vec}(\Phi_k) = r, \tag{40}$$

where each row in the matrix Z stores $2\mathfrak{Re}((\upsilon_{i1}^TA^TXK^{-1}) \otimes z_i^*)$. The condition $CB + B^TC^T > 0$ ensures that the transfer function $\Sigma_p(s)$ fulfils the required conditions of Theorem 3.1.

The determination of the location for new eigenvalues $j\omega_{i,p}$ is explained in Section IV-B in Grivet-Talocia (2004). Once Φ_k is constructed via (40), $\Phi = \Phi_k K^{-T}$ and $C_p = C + \Phi X^T$.

4.2 Pointwise-in-frequency scheme

The pointwise-in-frequency enforcement scheme proposed next is based on direct enforcement of the NI constraints at a few carefully selected frequency points. In this scheme, we solve (20) to obtain the maximum eigenvalue $\bar{\lambda}_i$ in the NI property violation frequency band (ω_i, ω_k). For $\bar{\lambda}_i > 0$, let the corresponding eigenvector of $H(j\omega_i)$ be ϑ_i. By applying a first-order eigenvalue perturbation analysis to $H(j\omega_i)$, we obtain

$$\hat{\bar{\lambda}}_i \simeq \bar{\lambda}_i + \vartheta_i^*(\delta H(j\omega_i))\vartheta_i, \tag{41}$$

where $\delta H(j\omega_i)$ is the matrix perturbation to $H(j\omega_i)$ that is required to displace $\bar{\lambda}_i$ to the new location $\hat{\bar{\lambda}}_i$.

Given $G = \left[\frac{A}{C}\middle|\frac{B}{D}\right]$ and $H(j\omega) = \frac{-j}{2}(G(j\omega) - G(j\omega)^*)$, let $G_p = \left[\frac{A}{C_p}\middle|\frac{B}{D}\right]$ and $H_p(j\omega) = \frac{-j}{2}(G_p(j\omega) - G_p(j\omega)^*)$. Defining $\Delta C = C_p - C$, we obtain $\delta G = G_p - G = \left[\frac{A}{\Delta C}\middle|\frac{B}{0}\right]$ and $\delta H = H_p - H = \frac{-j}{2}(\delta G_p(j\omega) - \delta G_p(j\omega)^*)$, and then (41) can be manipulated as follows:

$$\begin{aligned} \hat{\bar{\lambda}}_i &\simeq \bar{\lambda}_i + \vartheta_i^* \left(\frac{-j}{2}(\delta G(j\omega_i) - \delta G(j\omega_i)^*)\right)\vartheta_i \\ &= \bar{\lambda}_i + \vartheta_i^* \left(\frac{-j}{2}(\Delta C K_i - K_i^* \Delta C^T)\right)\vartheta_i \\ &= \bar{\lambda}_i + \frac{-j}{2}(\vartheta_i^* \Delta C K_i \vartheta_i - \vartheta_i^* K_i^* \Delta C^T \vartheta_i) \end{aligned}$$

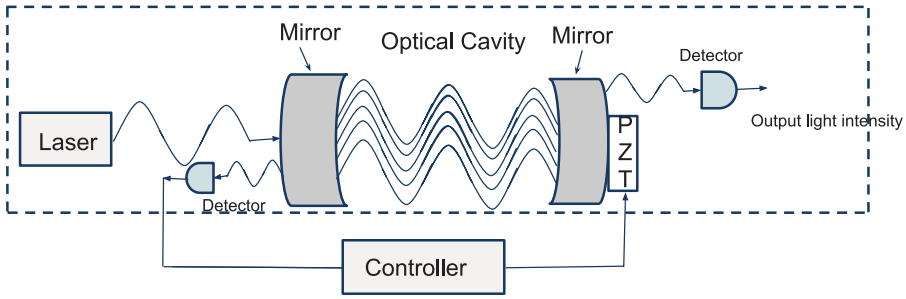

Figure 3. Cavity ring-down spectroscopy: block diagram.

$$
\begin{aligned}
&= \bar{\lambda_i} + \frac{-j}{2}(2j\Im\mathfrak{m}(\vartheta_i^* \Delta C K_i \vartheta_i)) \\
&= \bar{\lambda_i} + \Im\mathfrak{m}(\vartheta_i^* \Delta C K_i \vartheta_i) \\
&= \bar{\lambda_i} + \Im\mathfrak{m}(\mathrm{vec}(\vartheta_i^* \Delta C K_i \vartheta_i)) \\
&= \bar{\lambda_i} + \Im\mathfrak{m}((K_i\vartheta_i)^T \bigotimes \vartheta_i^*)\mathrm{vec}(\Delta C), \qquad (42)
\end{aligned}
$$

where $K_i = (j\omega_i I - A)^{-1}B$. Since the main goal is to have the new eigenvalue $\hat{\bar{\lambda}}_i \leq 0$ in the NI case and $\hat{\bar{\lambda}}_i < 0$ in the SNI case, this implies that (42) leads to the following linear inequality constraint:

$$
\mathrm{Im}((K_i\vartheta_i)^T \bigotimes \vartheta_i^*)\mathrm{vec}(\Delta C) \leq -\bar{\lambda_i}. \qquad (43)
$$

Also, in addition to the constraint (43), minimising the matrix norm $\|\Delta C\|$ leads to the following optimisation problem:

$$
\min \parallel \Delta C \parallel : \ \mathrm{Im}((K_i\vartheta_i)^T \bigotimes \vartheta_i^*)\mathrm{vec}(\Delta C) \leq -\bar{\lambda_i}. \qquad (44)
$$

Note that the inequality $\leq$ in (43) and (44) can be chosen as a strict inequality $<$ to enforce SNI models or to account for the approximation in (41).

By solving the optimisation problem (44), the minimum ΔC that enforces the system model to satisfy the NI property can be determined.

5. Application to a system arising in cavity ring down spectroscopy

This section presents an application of the NI enforcement schemes to a practical system arising in cavity ring down spectroscopy (CRDS). CRDS is a cavity-enhanced spectroscopic technique that works by injecting tunable coherent light from a laser source or a nonlinear optical device (either pulsed or continuous-wave) into a resonant optical cavity containing two or more highly reflective mirrors; see e.g. O'Keefe and Deacon (1988).

5.1 Experimental set-up

The experimental set-up for the system considered in this paper is depicted in Figure 3. Here, a Fabry–Perot optical cavity is used, which consists of a hollow tube fitted with two mirrors. For maximum constructive interference, the frequency of the laser light incident on the cavity must be the same as the cavity's resonant frequency. In such a case, the cavity is said to be in lock with input laser frequency. Any deviation between these frequencies is an undesired effect and is characterised in terms of a detuning parameter Δ. In order to maintain cavity lock, the resonant frequency of the cavity is varied by changing the distance between the mirrors in order to match the frequency of the input laser. This is achieved via a piezo-electric transducer (PZT) mounted on one of the mirrors, controlled using a suitable controller. The PZT in this system is an actuator collocated with the cavity which is the equivalent of a position sensor. Hence, as discussed is Section 1 the plant transfer function in this cavity system should be NI. The CRDS technique operates by injecting light into the optical cavity and by calculating the intensity of light at the output of the cavity using a suitable detector. For a detailed description of the experimental set-up, see Kallapur, Boyson, Petersen, and Harb (2011a, 2011b).

5.2 System model

A stable model for the plant corresponding to the Fabry–Perot cavity system was obtained using an iterative prediction-error method (PEM) applied to the measured frequency response data. The resulting state-space model was found to be

$$
A = \begin{bmatrix} -73280 & -3783 \times 10^4 & -1655 \times 10^9 \\ 1 & 0 & 0 \\ 0 & 1 & 0 \end{bmatrix},
$$

$$
B = \begin{bmatrix} 1 \\ 0 \\ 0 \end{bmatrix},
$$

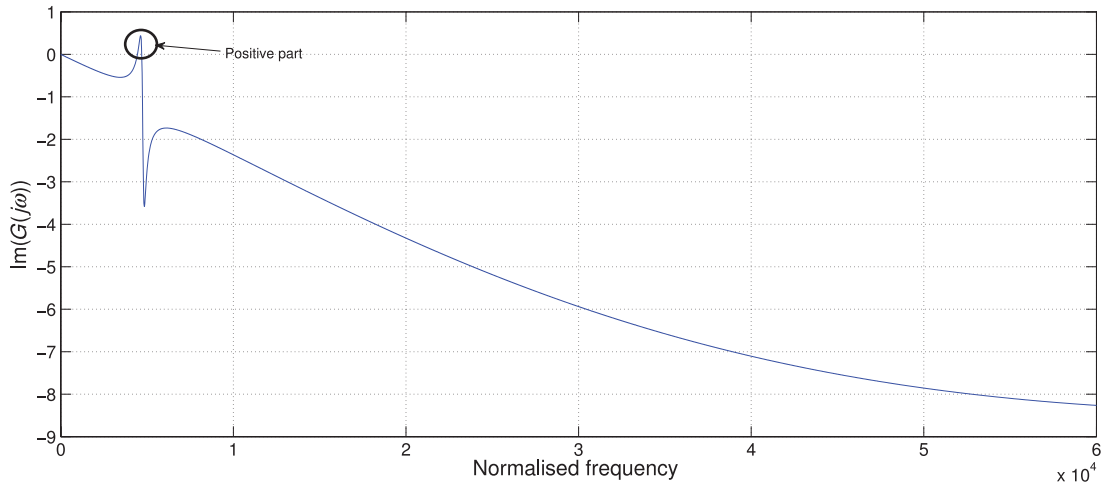

Figure 4. The imaginary part of the transfer function $G(j\omega)$.

$$C = \begin{bmatrix} 1230 \times 10^3 & 3151 \times 10^5 & 2791 \times 10^{10} \end{bmatrix},$$
$$D = 0. \tag{45}$$

The corresponding system transfer function is given by

$$G(s) = \frac{1.23 \times 10^6 s^2 + 3.151 \times 10^8 s + 2.791 \times 10^{13}}{s^3 + 7.328 \times 10^4 s^2 + 3.783 \times 10^7 s + 1.655 \times 10^{12}}. \tag{46}$$

A plot of the imaginary part of $G(j\omega)$ is presented in Figure 4. As seen from this plot, $G(j\omega)$ is NI except in the frequency band (4442.1518, 4692.0738). In Section 5.3, we apply the method outlined in Section 4.1 in order to enforce NI properties for all $\omega \in (0, \infty)$ on the mathematical model with transfer function (46).

5.3 *Plant model obtained using NI enforcement*

To find a plant model which is NI, we first need to compute the pure imaginary axis eigenvalues of the Hamiltonian matrix N_δ in (2) at $\delta = 0$. The Hamiltonian matrix N_0 for the given system has pure imaginary axis eigenvalues on the positive frequency branch at $\omega_0 = 0$, $\omega_1 = 4442.1518$ and $\omega_2 = 4692.0738$. We then apply the algorithm outlined in Section 4.1 in order to obtain a new plant model for the system described in (47) such that it is NI for

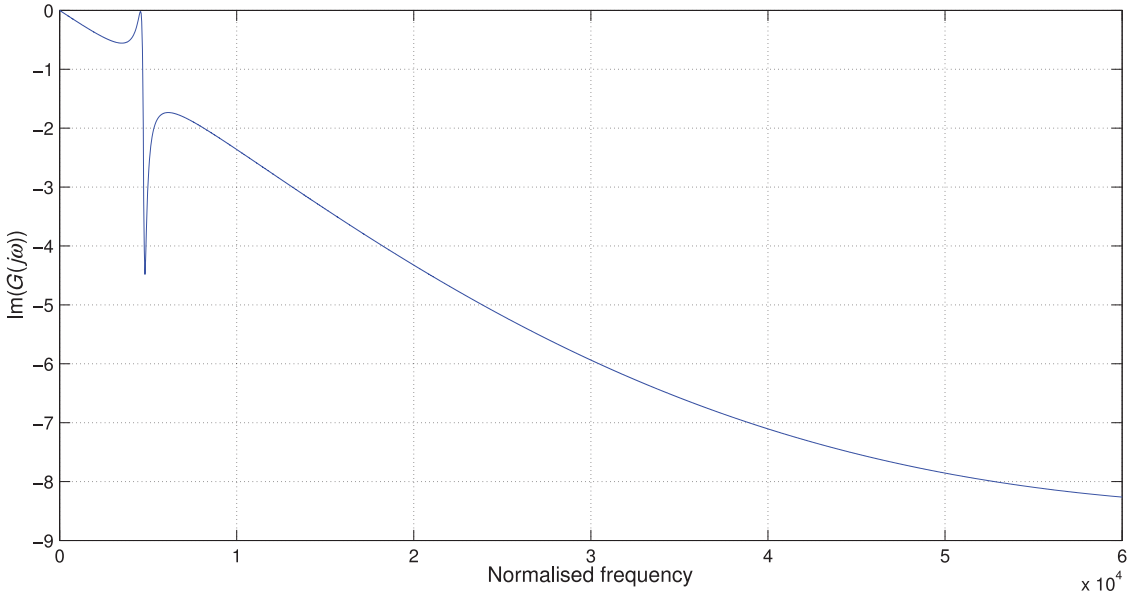

Figure 5. The imaginary part of the transfer function $G_p(j\omega)$ after enforcing the system to be NI.

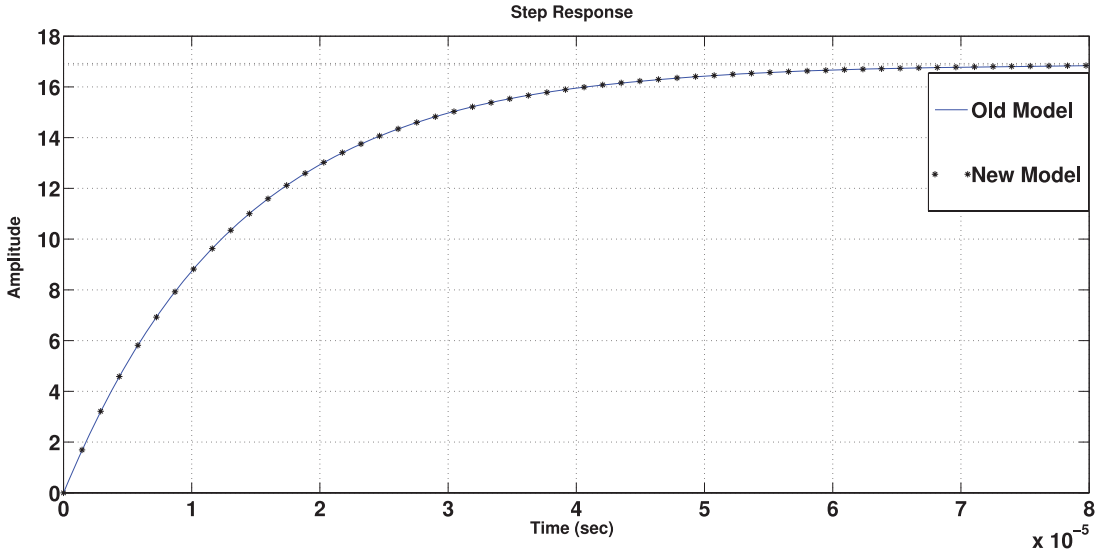

Figure 6. The step responses for $G(j\omega)$ and $G_p(j\omega)$.

$\omega \in (0, \infty)$. The state-space form for this model is given by

$$A = \begin{bmatrix} -73280 & -3783 \times 10^4 & -1655 \times 10^9 \\ 1 & 0 & 0 \\ 0 & 1 & 0 \end{bmatrix},$$

$$B = \begin{bmatrix} 1 \\ 0 \\ 0 \end{bmatrix},$$

$$C = \begin{bmatrix} 1230 \times 10^3 & 3151 \times 10^5 & 2801 \times 10^{10} \end{bmatrix},$$

$$D = 0. \tag{47}$$

Note that only the C matrix has changed. The corresponding system transfer function is given by

$$G_p(s) = \frac{1.23 \times 10^6 s^2 + 3.151 \times 10^8 s + 2.801 \times 10^{13}}{s^3 + 7.328 \times 10^4 s^2 + 3.783 \times 10^7 s + 1.655 \times 10^{12}}. \tag{48}$$

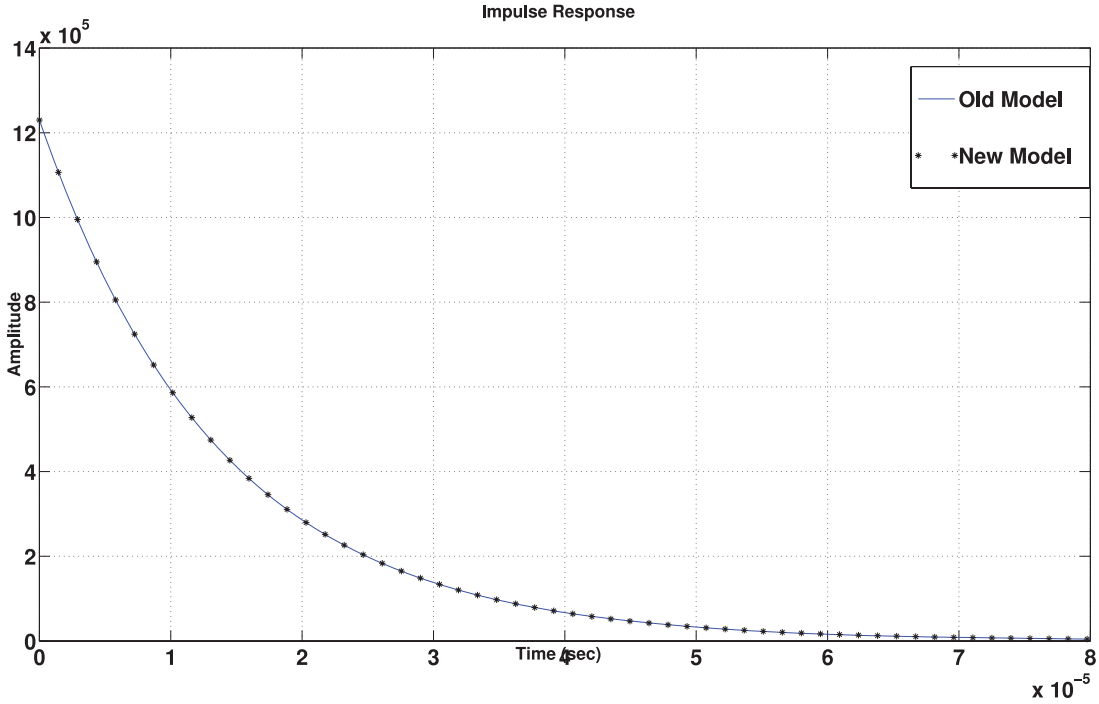

Figure 7. The impulse responses for $G(j\omega)$ and $G_p(j\omega)$.

The imaginary part of the transfer function for the perturbed system, $G_p(j\omega)$, is plotted in Figure 5 which shows that the model is indeed NI for $\omega \in (0, \infty)$.

Finally, we plot the step and impulse responses for $G(j\omega)$ in (46) as well as the modified model $G_p(j\omega)$ in (48), as shown in Figures 6 and 7, respectively. As seen from these graphs, both models exhibit similar responses, validating the enforcement process described in the paper.

6. Conclusion

In this paper, we have developed two methods that allow for perturbation of a mathematical system model to satisfy the NI properties. This was achieved by considering spectral perturbations of certain Hamiltonian matrices associated with the system and direct perturbation at a selected frequency of the system. The main results of this paper were based on the assumption that the pure imaginary axis eigenvalues of the system Hamiltonian matrix were simple and characterised by complete sets of eigenvectors. The methods outlined in this paper were applied to a plant model arising in an experimental Fabry–Perot cavity used in CRDS. It was shown that an NI system model for the plant could be obtained by perturbing the matrix C in its state-space representation (A, B, C, D).

For applications with non-simple eigenvalues, the results of the Hamiltonian matrix perturbation technique presented in this paper are not to be applicable. In such cases, further investigations are needed for the precise characterisation of NI violations.

Acknowledgements

The authors wish to thank Toby Boyson and Charles Harb from the University of New South Wales at the Australian Defence Force Academy for providing the frequency response data for the CRDS system. This work was supported by the Australian Research Council and the Engineering and Physical Sciences Research Council.

References

Anderson, B.D.O., & Vongpanitlerd, S. (1973). *Network analysis and synthesis: A modern systems approach*. Englewood Cliffs, NJ: Prentice-Hall.

Angeli, D. (2006). Systems with counterclockwise input-output dynamics. *IEEE Transactions on Automatic Control*, *51*, 1130–1143.

Bhikkaji, B., & Moheimani, S. (2009). Fast scanning using piezoelectric tube nanopositioners: A negative imaginary approach. *Proceedings of IEEE/ASME International Conference on Advanced Intelligent Mechatronics AIM* (pp. 274–279). July, Singapore: IEEE.

Brockett, R. (1970). *Finite dimensional linear systems*. New York: Wiley.

Brogliato, B., Lozano, R., Maschke, B., & Egeland, O. (2007). *Dissipative systems analysis and control* (2nd ed.). Communications and Control Engineering. London: Springer.

Cai, C., & Hagen, G. (2010 August). 'Stability analysis for a string of coupled stable subsystems with negative imaginary frequency response. *IEEE Transactions on Automatic Control*, *55*, 1958–1963.

Chinea, A., & Grivet-Talocia, S. (2007). A passivity enforcement scheme for delay-based transmission line macromodels. *IEEE Microwave Theory and Wireless Component Letters*, *17*, 562–564.

Chinea, A., & Grivet-Talocia, S. (2008). Perturbation schemes for passivity enforcement of delay-based transmission line macromodels. *IEEE Transactions on Advanced Packaging*, *31*, 568–578.

Devasia, S., Eleftheriou, E., & Moheimani, S.O.R. (2007). A survey of control issues in nanopositioning. *IEEE Transactions on Control Systems Technology*, *15*, 802–823.

Diaz, I.M., Pereira, E., & Reynolds, P. (2012). Integral resonant control scheme for cancelling human-induced vibrations in light-weight pedestrian structures. *Structural Control and Health Monitoring*, *19*, 55–69.

Dong, J., Salapaka, S.M., & Ferreira, P.M. (2007). Robust MIMO control of a parallel kinematics nano-positioner for high resolution high bandwidth tracking and repetitive tasks. *Proceedings of the 46th IEEE Conference on Decision and Control* (pp. 4495–4500). December, New Orleans, LA: IEEE.

El Rifai, K., El Rifai, O., & Youcef-Toumi, K. (2004). On dual actuation in atomic force microscopes. *Proceedings of the American Control Conference*, Vol. 4 (pp. 3128–3133).

Engelken, S., Patra, S., Lanzon, A., & Petersen, I.R. (2010). Stability analysis of negative imaginary systems with real parametric uncertainty – the SISO case. *IET Control Theory and Applications*, *4*, 2631–2638.

Fanson, J.L., & Caughley, T.K. (1990). Positive position feedback control for large space structures. *AIAA Journal*, *28*, 717–724.

Grasselli, O.M., & Longhi, S. (1991). Robust output regulation under uncertainties of physical parameters. *Systems and Control Letters*, *16*, 33–40.

Grasselli, O.M., Longhi, S., & Tornambe, A. (1993). Robust tracking and performance for multivariable systems under physical parameter uncertainties. *Automatica*, *29*, 169–179.

Grasselli, O.M., Longhi, S., Tornambe, A., & Valigi, P. (1996). Robust ripple-free regulation and tracking for parameter-dependent sampled-data systems. *IEEE Transactions on Automatic Control*, *41*, 1031–1037.

Grivet-Talocia, S. (2004). Passivity enforcement via perturbation of Hamiltonian matrices. *IEEE Transactions on Circuits and Systems*, *51*, 1755–1769.

Grivet-Talocia, S., & Ubolli, A. (2008). A comparative study of passivity enforcement schemes for linear lumped macromodels. *IEEE Transactions on Advanced Packaging*, *31*, 673–683.

Kallapur, A.G., Boyson, T.K., Petersen, I.R., & Harb, C.C. (2011a). Nonlinear estimation of ring-down time for a Fabry-Perot optical cavity. *Opt Express*, *19*, 6377–6386.

Kallapur, A.G., Boyson, T.K., Petersen, I.R., & Harb, C.C. (2011b). Offline estimation of ring-down time for an experimental Fabry-Perot optical cavity. *Proceedings of the IEEE International Conference in Control Applications (CCA)* (pp. 556–560). September, Denver, CO: IEEE.

Lanzon, A., & Petersen, I.R. (2007). A modified positive-real type stability condition. *Proceedings of the European Control Conference* (pp. 3912–3918). July, Kos, Greece: IEEE.

Lanzon, A., & Petersen, I.R. (2008). Stability robustness of a feedback interconnection of systems with negative imaginary frequency response. *IEEE Transactions on Automatic Control*, *53*, 1042–1046.

Lanzon, A., Song, Z., Patra, S., & Petersen, I.R. (2011). A strongly strict negative-imaginary lemma for non-minimal linear

systems. *Communications in Information and Systems*, *11*(2), 139–152.

Messenger, R.K., Aten, Q.T., McLain, T.W., & Howell, L.L. (2009). Piezoresistive feedback control of a MEMS thermal actuator. *Journal of Microelectromechanical Systems*, *18*, 1267–1278.

Michellod, Y., Mullhaupt, P., & Gillet, D. (2006). Strategy for the control of a dual-stage nano-positioning system with a single metrology. *Proceedings of the IEEE Conference Robotics, Automation and Mechatronics* (pp. 1–8). June, Bangkok: IEEE.

Moheimani, S.O.R., Vautier, B.J.G., & Bhikkaji, B. (2006). Experimental implementation of extended multivariable PPF control on an active structure. *IEEE Transactions on Control Systems Technology*, *14*, 443–455.

O'Keefe, & Deacon, A. (1988). Cavity ring-down optical spectrometer for absorption measurements using pulsed laser sources. *Review of Scientific Instruments*, *59*, 2544–2551.

Opmeer, M.R. (2011). Infinite-dimensional negative imaginary systems. *IEEE Transactions on Automatic Control*, *56*, 2973–2976.

Patra, S., & Lanzon, A. (2011). Stability analysis of interconnected systems with mixed negative-imaginary and small-gain properties. *IEEE Transactions on Automatic Control*, *56*, 1395–1400.

Petersen, I.R., & Lanzon, A. (2010). Feedback control of negative imaginary systems. *IEEE Control System Magazine*, *30*, 54–72.

Salapaka, S., Sebastian, A., Cleveland, J.P., & Salapaka, M.V. (2002). High bandwidth nano-positioner: A robust control approach. *Review of Scientific Instruments*, *73*, 3232–3241.

Sebastian, A., & Salapaka, S.M. (2005). Design methodologies for robust nano-positioning. *IEEE Transactions on Control Systems Technology*, *13*, 868–876.

Song, Z., Lanzon, A., Patra, S., & Petersen, I.R. (2012). A negative-imaginary lemma without minimality assumptions and robust state-feedback synthesis for uncertain negative-imaginary systems. *Systems & Control Letters*, *61*, 1269–1276.

van der Schaft, A. (2011). Positive feedback interconnection of Hamiltonian systems. *Proceedings of the 50th IEEE Conference on Decision and Control and European Control Conference (CDC-ECC)*, December, Orlando, FL, USA: IEEE.

van Hulzen, J.R., Schitter, G., Van den Hof, P.M.J., & van Eijk, J. (2010). Modal actuation for high bandwidth nano-positioning. *Proceedings of the American Control Conference* (pp. 6525–6530). July, Baltimore, Maryland, USA: IEEE.

Xiong, J., Petersen, I.R., & Lanzon, A. (2010). A negative imaginary lemma and the stability of interconnections of linear negative imaginary systems. *IEEE Transactions on Automatic Control*, *55*, 2342–2347.

Xiong, J., Petersen, I.R., & Lanzon, A. (2012). Finite frequency negative imaginary systems. *IEEE Transactions on Automatic Control*, *57*, 2917–2922.

Yong, Y.K., Ahmed, B., & Moheimani, S.O.R. (2010 March). Atomic force microscopy with a 12-electrode piezoelectric tube scanner. *Review of Scientific Instruments*, *81*, 033701.